

# Semi-Autonomous Surgical Robot Control for Beating-Heart Surgery

Lingbo Cheng\*, *Student Member, IEEE*, Jason Fong, Mahdi Tavakoli, *Member, IEEE*

**Abstract—** In this paper, a semi-autonomous robot control system is developed for 3D robotic tracking of the complex physiological organ motion introduced by respiration and heartbeat in cardiac surgery. The same control system enables the surgeon's hand to perceive the non-oscillatory portion of the surgical robot-heart tissue interaction force. The semi-autonomous surgical system includes a slave surgical robot which can compensate for the physiological organ motion automatically and a master robot (user interface) which is manipulated by the surgeon to provide task commands to the surgical robot. The proposed impedance control method for the surgical robot only needs the frequency range of the physiological motion to synchronize the surgical instrument with the organ motion automatically. Another reference impedance model for the master robot is designed to provide non-oscillatory force feedback to the surgeon. A usability study emulating the motion requirements of tissue ablation is carried out. Experimental results are presented to show the effectiveness of the proposed method by comparing the results to the manual compensation method.

## I. INTRODUCTION

Surgical robotics is a growing sector of the healthcare industry as it can extend the human operator's (the surgeon's) capabilities in various complex medical procedures, achieve precise system performance and patient safety, and benefit from a high degree of automation. Specifically, by using several sensors the assistive surgical robot will be much easier to acquire data and/or images during a surgical procedure. Also, the implementation of a computer vision system makes it possible for the surgical automation to understand how and where to navigate the surgical instruments with a high level of accuracy during the operation.

An important application of surgical robotic systems is beating-heart surgery, which has many advantages over the conventional stabilized-heart surgery such as enabling intraoperative evaluation of the heart (which in turn will improve patient outcomes and shorten lengths of stay) and eliminating the negative effects of stabilized-heart surgery [1].

In beating-heart surgery, motions induced by respiration and heartbeat represent a source of perturbation in the surgical maneuvers, which makes the surgical instrument control under physiological organ motion challenging. As manually compensating for such motions is difficult for the human operator, an automated surgical instrument will be helpful to

compensate for the complex organ motion. However, a surgical robot with too much autonomy can increase the risk of injuring the patient as a medical tool operating under feedback control is vulnerable to various sources of disturbances, inaccuracies and uncertainties [2]. Therefore, in this paper, a semi-automated surgical robot control system is considered and proposed, where the surgical tool is synchronized with the beating-heart motion automatically to give the human operator a feeling of operating on a seemingly stabilized heart while the specific operations are performed by the human operator.

Another issue for the semi-autonomous surgical robot system is haptic feedback for the human operator. As the human operator cannot touch the beating-heart tissue directly when using the robotics assistance, appropriate haptic feedback is necessary to reduce tissue damages and undesirable trauma. While synchronizing the surgical robot's motions with the beating-heart motions causes the force sensor attached to the surgical robot to register forces due to the force sensor inertia, these forces should not be transmitted to the human operator. Indeed, the ideal haptic feedback for the human operator is the non-oscillatory haptic feedback that is due to the interaction between the surgical robot and the heart.

To address the issue of automatic motion compensation for the physiological organ motion, in [3] and [4], the authors used ultrasound imaging to detect the position of the beating-heart tissue as the reference for the surgical robot's position. In [5], a force control scheme was proposed to compensate for the physiological motion by using a viscoelastic active observer. In [6], a conventional inner force feedback control loop and an out control loop based on iterative learning control were proposed for the compensation of periodic organ motion. Also, in [7], the authors combined the ultrasound-guided visual servoing and an admittance force controller to achieve moving kidney stones tracking. These work focused on single robot systems instead of telerobotic systems which can enable motion/force scaling and remote manipulation [8]. In bilateral teleoperation systems, haptic feedback can be achieved so that the human operator can feel the environment (beating heart) force and effectively manipulate the master robot to provide appropriate position commands. In this paper, we are interested in using a bilateral teleoperation system to realize 3D physiological motion compensation and non-oscillatory force feedback to the human operator.

\*Corresponding author. The authors are with the Department of Electrical and Computer Engineering, University of Alberta, Edmonton, AB T6G 1H9, Canada. (e-mails: [lingbo1@ualberta.ca](mailto:lingbo1@ualberta.ca), [mahdi.tavakoli@ualberta.ca](mailto:mahdi.tavakoli@ualberta.ca)).

Among the proposed telerobotic systems for beating-heart motion compensation, position-based control systems are very common. The heart motion can be obtained through different sensors. In [9], a high-speed camera was employed to measure the heart motion. In [10], an infrared tracking approach was proposed by placing several markers on the heart surface. These approaches, however, are not suitable for intra-cardiac surgery. In [11], [12], the authors predicted the future heart motion via using two sonomicrometer crystals. The position where sonomicrometry crystals are placed can be measured. In addition, our group proposed a system that combines ultrasound imaging with a generalized predictive control algorithm to compensate for the heart's motion [13]–[15]. Although the use of ultrasound imaging extends the system's application to the interior heart surgery, low sampling rate of the ultrasound machine and time delays caused by ultrasound image acquisition and processing pose closed-loop system control challenges that we tackled. In [16], [17], we proposed an impedance-controlled method to enable the surgical robot have flexibility, so that motion compensation can be achieved. Also, to tackle the problems of oscillatory force feedback, in [18] a cascade model predictive control architecture with a Kalman active observer was employed. In [15]–[17], a reference impedance model was designed for the master robot to provide non-oscillatory force feedback.

Additionally, in realistic beating-heart surgery, visual stabilization when displaying images of the beating heart to the human operator is another important issue. It should not only compensate for the heart's motion but should also compensate for tissue deformations. As this research focuses on motion compensation and force feedback, visual stabilization is accomplished by using an eye-in-hand configuration [19] for the camera and the heart simulator instead of using the existing 3D tracking algorithms [20]. The camera can obtain a stabilized view of the beating heart by moving with the heart.

In this paper, the developed semi-autonomous surgical robot control system for beating-heart surgery utilizes an impedance-controlled teleoperation framework (Fig. 1) which includes a master robot in the local site and a slave robot (surgical robot) in the remote site to achieve the desired

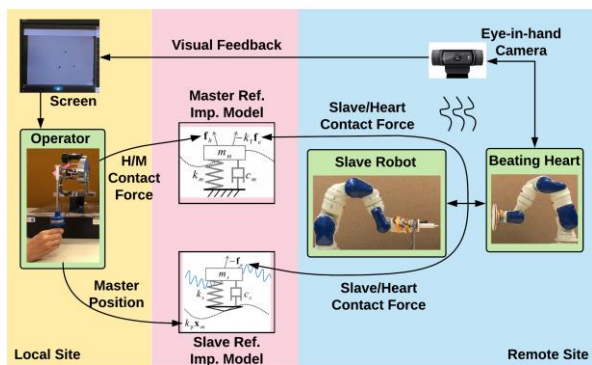


Figure 1. A schematic of the proposed semi-autonomous surgical robot control system for beating-heart surgery. The human operator manipulates the master robot in the local site and provides position commands for the slave robot in the remote site. Two 7-DOF Motoman SIA5F robots are used as the slave robot and the simulated beating heart, respectively. A camera mounted on the end of the heart simulator is used to provide stabilized view of the beating heart to the human operator. H/M contact force is the abbreviation of human-master contact force.

objectives. Two reference impedance models for the master and slave robots, respectively, are designed, and the results for a 3D task to be done on a simulated heart undergoing a 3D motion are presented. The 3D motion trajectory of the simulated heart was extracted from a real heart's motion (courtesy of the authors of [21] who provided us with the data). A 7-DOF Motoman SIA5F robot with significant dynamics, which is more similar to a real surgical robot, is used as the slave robot.

The main advantage of the proposed method over the previous methods is the simplicity of the external sensor system which only involves two force sensors to record contact forces. With no need for organ motion prediction, observation or learning, the developed system can achieve physiological organ motion compensation and non-oscillatory haptic feedback simultaneously. Moreover, this system can be used for surgeries with heart arrhythmia as well.

The proposed reference impedance models for the master and slave robots build on previous work of the authors [16] and extend the previous 1D task on a simulated heart undergoing a 1D motion to a 3D task on a simulated heart undergoing a real 3D heart motion. Relative to the past work, the main contributions of this paper are therefore as follows: (a) Considering a more complicated 3D physiological heart motion (includes breathing motion and heartbeat motion) instead of the simulated 1D heart motion generated by a custom-built mechanical cam is used for motion compensation, (b) using a 7-DOF Motoman SIA5F robot with significant dynamics, which is more similar to a real surgical robot, is used as the slave robot, whereas in [16], a haptic device with negligible dynamics was used as the slave robot, (c) investigating whether the parameters of the slave impedance model can be tuned to the appropriate values given the significant dynamics of the Motoman SIA5F robot (in our previous work the parameters of the slave impedance model could be freely adjusted anywhere from near zero to infinity), (d) using a different controller for the slave robot, 7-DOF Motoman SIA5F robot, which requires movements to be performed through a velocity controller as opposed to a position controller for haptic devices, and (e) considering a 3D task is performed in the usability study to emulate the motion requirements of tissue ablation, while in the previous work only a 1D anchor deployment was performed. The contributions of this paper lay the foundation for the future implementation of even more complex experiments using more actual surgical robotic systems. Furthermore, the proposed system is suitable for cardiac surgeries with arrhythmia which is more challenging for motion prediction methods.

The paper is organized as follows. Section II introduces the developed system. Section III presents the control algorithms for the robots. Section IV shows the experimental results, usability study, and discussion. Finally, Section V concludes the paper.

## II. SEMI-AUTONOMOUS SURGICAL ROBOT CONTROL SYSTEM FOR BEATING-HEART SURGERY

The developed semi-autonomous surgical robot control system for beating-heart surgery involves a master robot that provides position commands and a slave robot that receives

those commands and executes tasks on the beating-heart tissue. In our developed system, two force sensors are mounted on the end of the master and slave robots, respectively. A thin rigid surgical tool is used as the end-effector of the slave robot. By utilizing the measured interaction forces, the synchronization with the physiological organ motion for the slave robot and the non-oscillatory force feedback for the master robot can be achieved simultaneously.

The surgical procedure has two phases: No contact with the heart and contact with the heart. A force sensor mounted on the end-effector of the slave robot can be used to distinguish the two phases. When there is no contact between the beating heart and the slave robot, the slave robot should follow the (possibly scaled) trajectory of the master robot. When contact occurs, the slave robot should synchronize its motions with the heart's motion and execute desired surgical tasks on the heart tissue. At the same time, the operator should only perceive the non-oscillatory haptic feedback.

Indeed, the proposed system and strategy will be more suitable for surgical applications that need low and constant contact forces between the surgical instruments and the tissue such as cardiac ablation. To be more specific, for tissue ablation, it is extremely important to control the tool-tissue contact force within a safe range to minimize tissue damage. Any unsteady operation of the human operator may increase the risk of tissue damage. Therefore, the main desired objectives of the system during tool-tissue contact are motion compensation and non-oscillatory haptic feedback. In other words, during tissue ablation, the surgical instrument should synchronize with the heart tissue first instead of following the exact position commands of the human operator, and at the same time, to provide the operator with a steady operation feeling, non-oscillatory haptic feedback is needed.

Fig. 2 shows the teleoperation scheme, which includes four main blocks: the human operator, the beating heart, the master robotic system, and the slave robotic system. By transmitting the force and position information of the master and slave robots through the communication channel, we proposed the reference impedance models for the master and slave robots, respectively, which are described in detail in Section III.

In Fig. 2,  $\mathbf{f}_h$  is the interaction force between the master robot and the human operator, and  $\mathbf{f}_e$  is the interaction force

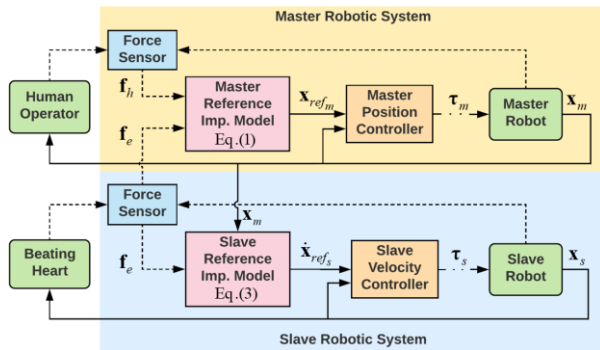


Figure 2. The telerobotic beating-heart surgical system with motion compensation models and force feedback. The solid lines indicate the position transfer paths. The dashed lines indicate the force transfer paths. The dash-dotted lines are control signals.

between the slave robot and the beating heart. They are measured directly through two force sensors. The desired position for the master robot,  $\mathbf{x}_{ref_m}$ , and the desired velocity for the slave robot,  $\dot{\mathbf{x}}_{ref_s}$ , are generated by the reference impedance models for the respective robots. The actual positions of the master and slave robots are  $\mathbf{x}_m$  and  $\mathbf{x}_s$ , respectively. The controllers receive the desired position and velocity generated by the reference impedance models, and output torques  $\boldsymbol{\tau}_m$  and  $\boldsymbol{\tau}_s$  to the robots. The position controller for the master robot and the velocity controller for the slave robot are described in Section III.

### III. CONTROL ALGORITHMS

Algorithms presented in this section will focus on the reference impedance models for the master and slave robots and the parameter adjustment guidelines for the impedance models. The two reference impedance models are described in Section III-A, and the tuned parameters of the models are presented in Section III-C based on the recorded 3D beating-heart motion signals presented in Section III-B. The controllers for the master and slave robots are described in Section III-D.

#### A. Reference Impedance Models

The reference impedance model for the master robot in Cartesian coordinates includes the human-master interaction force, the scaled slave-heart interaction force, and the desired master response trajectory. The relationships can be expressed as

$$\mathbf{M}_m \ddot{\mathbf{x}}_{ref_m} + \mathbf{C}_m \dot{\mathbf{x}}_{ref_m} + \mathbf{K}_m \mathbf{x}_{ref_m} = \mathbf{f}_h - \mathbf{K}_f \mathbf{f}_e \quad (1)$$

where  $\mathbf{K}_m$ ,  $\mathbf{C}_m$ ,  $\mathbf{M}_m$  are the virtual stiffness, damping and mass 3-by-3 diagonal matrices of the master impedance model. Also,  $\mathbf{K}_f$  is a diagonal matrix of the force scaling factor. The interaction forces ( $\mathbf{f}_h \in \mathbb{R}^{3 \times 1}$ ,  $\mathbf{f}_e \in \mathbb{R}^{3 \times 1}$ ) and the desired master response ( $\mathbf{x}_{ref_m} \in \mathbb{R}^{3 \times 1}$ ) are vectors.

Equivalently, the transfer function of (1) in each axis can be written as a second order function with a damping ratio  $\zeta_{m_i}$  and a natural frequency  $\omega_{n_{m_i}}$

$$Z_{m_i} = \frac{1}{m_{m_i} s^2 + c_{m_i} s + k_{m_i}} = \frac{\omega_{n_{m_i}}^2}{k_{m_i} (s^2 + 2\zeta_{m_i} \omega_{n_{m_i}} s + \omega_{n_{m_i}}^2)} \quad (2)$$

where  $\zeta_{m_i} = \frac{c_{m_i}}{2\sqrt{m_{m_i} k_{m_i}}}$  and  $\omega_{n_{m_i}} = \sqrt{\frac{k_{m_i}}{m_{m_i}}}$ . Note that  $i = x, y, z$  for the  $x$ -,  $y$ -,  $z$ -axis, respectively.

Correspondingly, matrix  $\mathbf{M}_m = \text{diag}(m_{m_x}, m_{m_y}, m_{m_z})$ ,  $\mathbf{C}_m = \text{diag}(c_{m_x}, c_{m_y}, c_{m_z})$ ,  $\mathbf{K}_m = \text{diag}(k_{m_x}, k_{m_y}, k_{m_z})$ ,  $\boldsymbol{\Xi}_m = \text{diag}(\zeta_{m_x}, \zeta_{m_y}, \zeta_{m_z})$ , and  $\boldsymbol{\Omega}_{n_m} = \text{diag}(\omega_{n_{m_x}}, \omega_{n_{m_y}}, \omega_{n_{m_z}})$ . In the following, only matrices  $\mathbf{K}_m$ ,  $\boldsymbol{\Xi}_m$ , and  $\boldsymbol{\Omega}_{n_m}$  will be adjusted.

The reference impedance model for the slave robot is concerned with the slave-heart interaction force and the desired slave impedance model's response deviation from the trajectory of the master robot. It can be expressed as

$$\mathbf{M}_s \ddot{\tilde{\mathbf{x}}}_{ref_s} + \mathbf{C}_s \dot{\tilde{\mathbf{x}}}_{ref_s} + \mathbf{K}_s \tilde{\mathbf{x}}_{ref_s} = -\mathbf{f}_e \quad (3)$$

where  $\tilde{\mathbf{x}}_{ref_s} = \mathbf{x}_{ref_s} - \mathbf{K}_p \mathbf{x}_m$ , and  $\mathbf{K}_p$  is a matrix of the position

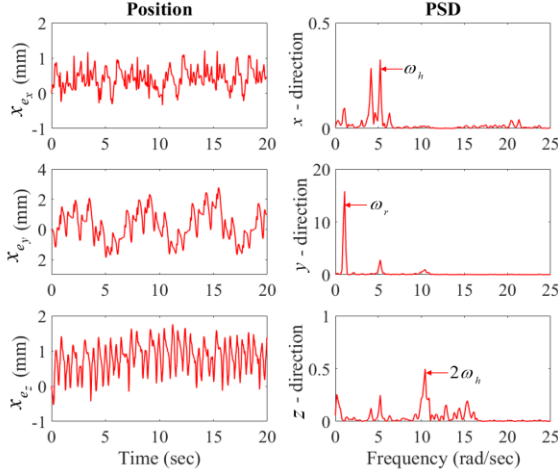


Figure 3. 3D heart motion measured from an *in vivo* porcine heart stereo video which recorded image sequence of a totally endoscopic coronary artery bypass graft from a daVinci (Intuitive Surgical, CA) surgical platform and its power spectral density (PSD) analysis.

scaling factor. Here,  $\mathbf{x}_m \in \mathbb{R}^{3 \times 1}$  is the vector of the master robot position. Also,  $\mathbf{K}_s$ ,  $\mathbf{C}_s$ ,  $\mathbf{M}_s$  are the virtual stiffness, damping and mass diagonal matrices of the slave impedance model.

The transfer function of (3) in each axis is

$$Z_{s_i} = \frac{1}{m_{s_i}s^2 + c_{s_i}s + k_{s_i}} = \frac{\omega_{n_{s_i}}^2}{k_{s_i}(s^2 + 2\omega_{n_{s_i}}s + \omega_{n_{s_i}}^2)} \quad (4)$$

where  $\zeta_{s_i} = \frac{c_{s_i}}{2\sqrt{m_{s_i}k_{s_i}}}$  and  $\omega_{n_{s_i}} = \sqrt{\frac{k_{s_i}}{m_{s_i}}}$ . Also,  $i = x, y, z$  for the  $x$ -,  $y$ -,  $z$ -axis, respectively. The matrices that need to be adjusted are  $\mathbf{K}_s = \text{diag}(k_{s_x}, k_{s_y}, k_{s_z})$ ,  $\mathbf{E}_s = \text{diag}(\zeta_{s_x}, \zeta_{s_y}, \zeta_{s_z})$ , and  $\mathbf{\Omega}_{n_s} = \text{diag}(\omega_{n_{s_x}}, \omega_{n_{s_y}}, \omega_{n_{s_z}})$ .

### B. Heart Motion

The motion of beating-heart surface is primarily induced by respiratory and heartbeat motions with different frequency ranges. In the paper, the 3D heart positions were measured offline from a stereo video of *in vivo* porcine heart by vision tracking [21]. The stereo video recorded image sequence of a totally endoscopic coronary artery bypass graft from a daVinci (Intuitive Surgical, CA) surgical platform [22]. The quasi-periodic 3D heart motion signals with the respective power spectral densities (PSD) are shown in Fig. 3. Observable dominant peaks are at  $\omega_r = 1.07$ ,  $\omega_h = 5.22$ , and  $2\omega_h = 10.43$  rad/sec, which correspond to respiratory motion, heartbeat motion, and the first harmonic of the heartbeat motion, respectively. These dominant frequencies will be used to adjust the parameters of the reference impedance models.

### C. Parameters Tuning

According to Section III-A, the matrices that need to be tuned are  $\mathbf{K}_m$ ,  $\mathbf{E}_m$ ,  $\mathbf{\Omega}_{n_m}$ , and  $\mathbf{K}_s$ ,  $\mathbf{E}_s$ ,  $\mathbf{\Omega}_{n_s}$ . For the sake of brevity, the parameters tuning guidance shown below is in one direction. The subscript  $i = x, y, z$  for the  $x$ -,  $y$ -,  $z$ -axis, respectively.

The reference impedance model for the master robot (1) aims to avoid possible fatigue and exhaustion caused by the oscillatory slave-heart interaction force feedback to the human operator. It means that the high frequency of the slave-heart

interaction force should be filtered to achieve  $(f_{h_i} - k_{f_i}f_{e_i}) \rightarrow 0$ . To satisfy this condition, the stiffness of model (1) ( $k_{m_i}$ ) should be chosen small, and the natural frequency of (1) ( $\omega_{n_{m_i}}$ ) should be several times smaller than the lower rate of the physiological motion; that is,  $\omega_{n_{m_i}} \ll \omega_r$  (Fig. 4a). Also, to get a fast behaviour in response to the harmonic physiological force of the human operator,  $\zeta_{m_i}$  is chosen to be 0.7.

The goal of the slave impedance model (3) is to make the slave robot comply with the physiological force and motion during tool-tissue interaction. Based on (3), the flexibility of the slave robot, which can neither be too small nor too large, is the deviation from the scaled master trajectory ( $\tilde{x}_{ref_{s_i}} = x_{ref_{s_i}} - k_{p_i}x_{m_i}$ ). If the slave robot is too flexible, it cannot apply enough forces on the heart surface to perform tasks. If the slave robot is too rigid, the motion compensation cannot be achieved. Therefore, the stiffness value of the slave impedance model ( $k_{s_i}$ ) should be adjusted to be moderate. The exact stiffness can be tuned by trial and error according to specific task and the used slave robot. Also, the natural frequency of (3) ( $\omega_{n_{s_i}}$ ) should be several times greater than the higher rate of the physiological motion ( $\omega_{n_{s_i}} \gg \omega_h$ ) (Fig. 4b). Similarly,  $\zeta_{s_i}$  is chosen to be 0.7.

It is worth noting that the flexibility of the slave robot may reduce the transparency of the system, but it is significantly important for heart motion compensation. For specific cardiac surgeries such as tissue ablation, to reduce the risk of tissue damage there is no need for the slave robot to track the exact scaled master robot's trajectory during operation. On the contrary, it is more important to synchronize the surgical instrument with the moving tissue and keep the contact force at a safe level. The affected transparency will lead to the master position tracking to be scaled again, which not only guarantees the motion compensation ability of the slave robot but also reduces the tissue damage risk. When there is no contact between the beating heart and slave robot, the slave robot will track the exact scaled position of the master robot

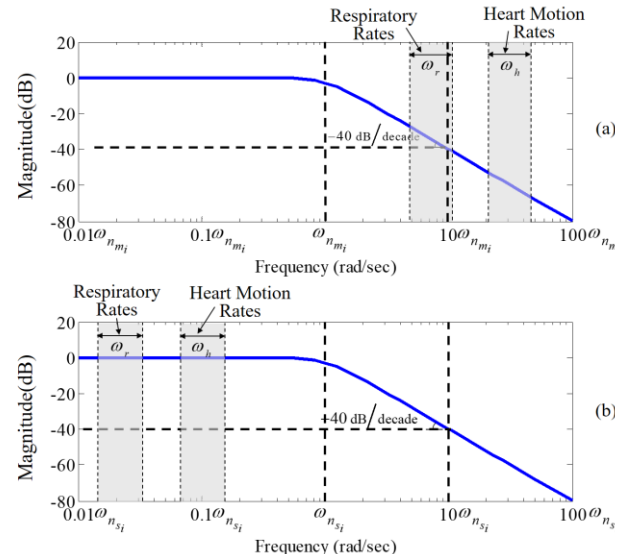


Figure 4. Bode diagrams in one direction of (a) the master reference impedance model and (b) the slave reference impedance model.

and the transparency of the system is good. Therefore, the trade-off between the transparency and the flexibility of the system makes the proposed strategy and parameter tuning guidelines more suitable for applications that need low and constant contact forces in beating-heart surgery.

#### D. Controllers

To track the ideal responses of the two reference impedance models for the master and slave robots, a proportional-integral-derivative (PID) controller is employed for the master robot. In the experiments, the proportional, integral, and derivative terms are set as  $\mathbf{K}_{p_m} = 1000\mathbf{I}_{3 \times 3}$ ,  $\mathbf{K}_{i_m} = 200\mathbf{I}_{3 \times 3}$ , and  $\mathbf{K}_{d_m} = \mathbf{I}_{3 \times 3}$ . Control of the slave robot is performed through a velocity controller as opposed to a position controller.

It is worth noting that the procedure explained above entails using the desired impedance surfaces (1) and (3) in an admittance control framework where based on measurements of contact forces  $\mathbf{f}_h$  and  $\mathbf{f}_e$ , a desired position for the master robot and a desired velocity for the slave robot are calculated and fed to respective position and velocity controllers [23]. Alternatively, we could have implemented an impedance controller on the slave robot for generating torque commands to ensure that (3) holds. However, in this case, the inverse dynamics of the slave robot would be required but they are unavailable due to the complexity in estimating the dynamics of the 7-DOF Motoman robot.

### IV. EXPERIMENTAL EVALUATION

Experiments are implemented with motion compensation (the proposed strategy) and without motion compensation (the direct-force-reflection haptic teleoperation control [24]). The experimental setup for the two cases is the same. The only difference between the two cases is the control method. The task requires a prolonged contact with the heart surface to evaluate the performance of position tracking and force feedback. Different from the proposed semi-autonomous control method, for the case without motion compensation, the operator must synchronize the slave robot with the heart motion manually and perform task on the heart tissue; that is, the simulated surgical operation is fully manual. The experimental results and a usability study emulating the motion requirements of tissue ablation are presented in Section IV-B and -C. The discussion is presented in Section IV-D.

#### A. Experimental Setup

The experiment employs a 3D Phantom Premium 1.5A robot (Geomagic Inc., Wilmington, MA, USA) equipped with a 6-DOF (degree of freedom) 50M31 force/torque sensor (JR3 Inc., Woodland, CA, USA) as the master robot and a Motoman SIA-5F (Yaskawa America, Inc., Miamisburg, OH, USA) 7-DOF serial manipulator equipped with a 6D ATI Gamma Net force/torque sensor (ATI Industrial Automation, Inc., Apex, NC, USA) as the slave robot (Fig. 5).

The encoder positions of the master and slave robots were transformed into end-effector positions and recorded. The beating-heart is simulated by another Motoman manipulator attached with a flat interface (a soft tissue phantom) and a camera to provide visual stabilization. The simulated heart tissue is made having a stiffness of 200 N/m to imitate the real

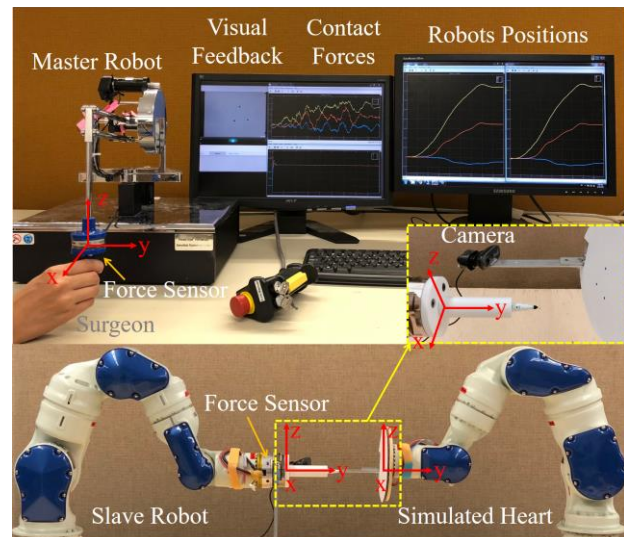


Figure 5. Experimental setup: master robot, slave robot and beating heart simulator. An eye-in-hand configuration for the camera and the beating heart simulator is used to accomplish visual stabilization.

heart tissue [25]. The whole system of the heart simulator was controlled to have a 3D movement by giving the recorded heart position signals as shown in Fig. 3. The QUARC software (Quanser Consulting Inc., Markham, ON, Canada) is used as a real-time control environment to implement the proposed method with a sampling rate of 1 kHz. The 3D heart position signals were interpolated from its inherent measurement rate which is 25 Hz to the sampling rate of 1 kHz. The MATLAB/SIMULINK program includes the master robot controller, the reference impedance models for the master and slave robots, and the UDP blocks to communicate between the Simulink based models and the C++ based velocity controller for the slave robot. The parameters of the impedance models are listed in Table I.

#### B. Experimental Results

The performance of the developed system is evaluated by calculating the mean absolute synchronization error (MASE) in 3D,  $MASE = \frac{1}{n} \sum_{i=1}^n |e_i|$ , where  $e_i$  is the position error in 3D between the surgical tool tip and its desired position when contact occurs,  $n$  is the samples number of contact duration. The contact between the slave robot and the heart tissue is detected based on the slave-heart interaction force. When no motion compensation provided, the desired trajectory is defined to be the heart position as the human operator is conducted to manually synchronize the slave robot with the heart motion and try to remain in contact on the surface of the heart. When motion compensation provided, the desired position for the slave robot is defined as the combined trajectory of the master robot and the heart. The experiments are carried out for 100 s. The first and last  $\sim 10$  s of the 100 s are used for the slave robot to approach and leave the heart. The position results are shown in Table II. In addition, the average force applied by the human operator on the master robot (AFM) in 3D and the average force applied by the slave robot on the simulated heart (AFS) in 3D are calculated and presented in Table II as well.

Table.I. PARAMETERS OF THE REFERENCE IMPEDANCE MODELS

Impedance Model (1)	Impedance Model (3)
$\mathbf{K}_m = \text{diag}(7.2, 2.7, 5) \text{ N/m}$	$\mathbf{K}_s = \text{diag}(125, 160, 250) \text{ N/m}$
$\mathbf{\Xi}_m = 0.7\mathbf{I}_{3 \times 3}$	$\mathbf{\Xi}_s = 0.7\mathbf{I}_{3 \times 3}$
$\mathbf{\Omega}_{n_m} = \text{diag}(0.6, 0.3, 0.5) \text{ rad/sec}$	$\mathbf{\Omega}_{n_s} = \text{diag}(25, 40, 50) \text{ rad/sec}$
$\mathbf{K}_f = \mathbf{I}_{3 \times 3}$	$\mathbf{K}_p = \mathbf{I}_{3 \times 3}$

Table.II. EXPERIMENTAL RESULTS

Motion Compensation	Yes	No
MASE (mm)	0.959	2.373
AFM (N)	$1.021 \pm 0.079$	$0.290 \pm 0.189$
AFS (N)	$0.791 \pm 0.181$	$0.290 \pm 0.189$

As can be seen in Table II, with motion compensation, the MASE is 0.959 mm which is much lower than the values when motion compensation is not provided (2.373 mm). It is worth noting that the MASE is higher than the value presented in [13]. However, this comparison is not appropriate as the experimental systems are totally different. In addition, in [13], the slave robot did not contact the simulated heart tissue, which further indicates that the two experiments are not suitable for comparison. Moreover, taking into consideration the significant dynamic of the surgical robot, this position tracking result is satisfied for now. Also, with motion compensation, the standard deviation of AFM (0.079 N) is much lower than the standard deviation of AFS (0.181 N), which means the force perceived by the human operator is steadier and the oscillatory portion of slave-heart contact forces is filtered out perfectly. Without motion compensation, as the slave-heart contact force is directly reflected to the human operator, the means and standard deviations of AFM and AFS are the same. Moreover, it is worth noting that the mean value of AFM with motion compensation (1.021 N) is higher than that without motion compensation (0.29 N). It is because that without motion compensation the human operator must manually synchronize the slave robot with the heart motion which results in contact discontinuity during operation as the slave robot has a high risk of bouncing off the heart surface.

Fig. 6 shows the actual slave robot positions and its desired trajectories in 3D for the cases with and without motion compensation. The right vertical axis of Fig. 6 is the position tracking error for each direction and each case. As can be seen more clearly in Fig. 6, the position tracking errors shown in Fig. 6(b) are much smaller than the errors shown in Fig. 6(a), which demonstrates that the motion compensation performance improves significantly by using the proposed semi-autonomous surgical robot control system.

Contact force results for each case in 3D are shown in Fig. 7. All three axes of the robots demonstrated similar performance. In Fig. 7(a), as the slave-heart contact force is directly reflected to the human operator, the force perceived by the human operator and the slave-heart contact force are the same. Due to the manual motion compensation and contact discontinuity, both are oscillatory and very low. In Fig. 7(b), the slave-heart contact force in each direction (blue dashed line) is always positive and higher than that in Fig. 7(a), which means the tool-heart contact is constant although the amplitude of the oscillatory portion of the slave-heart contact force still high. Also, in Fig. 7(b), the human-master contact forces (red

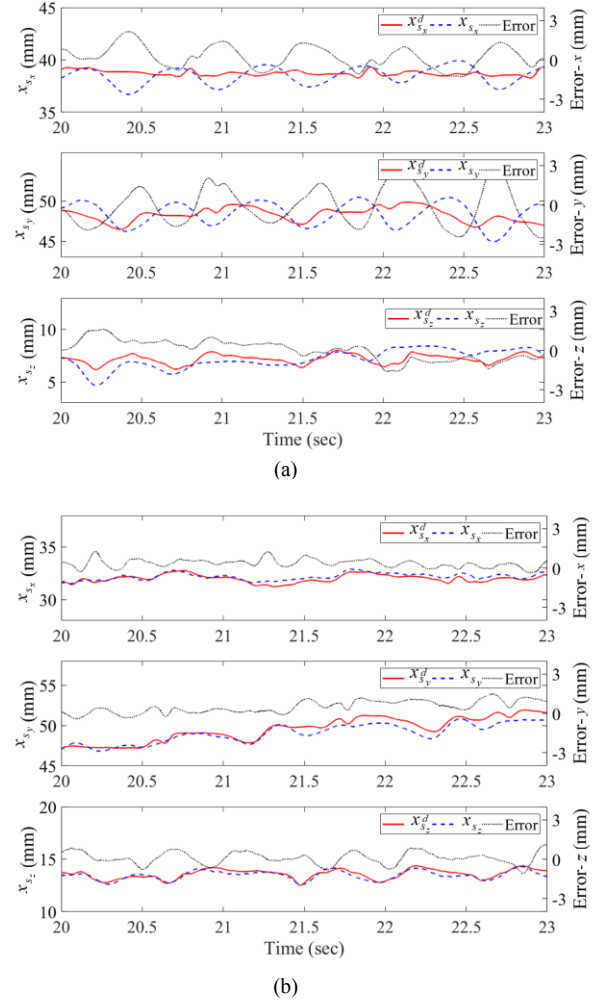


Figure 6. Results of the slave robot 3D position with its real (blue dashed line,  $x_{s_i}$ ) and desired (red solid line,  $x_{s_i}^d$ ) trajectories and tracking error (black dotted line) for the cases (a) without motion compensation and (b) with motion compensation. Subscripts  $i = x, y, z$  are the three axes, respectively.

solid line) are much steadier than the slave-heart contact forces as their oscillatory portions are filtered out by using the proposed method.

To further explore the difference between the two cases, the position and force results of the master robot in the  $y$ -axis for each case are presented in Fig. 8. With motion compensation, both position and force of the human operator are relatively steady which provides the human operator a feeling of operating on an ‘arrested’ heart.

### C. Usability Study

The usability study emulates the motion requirements of tissue ablation, which needs a prolonged contact with the heart surface. The task simulating this is to draw a triangle with sides that are 4 cm long on the surface of the simulated heart. The task starts at the left bottom of the triangle and proceeds in the clockwise direction. This study is completed with and without motion compensation by one user (the first author). For each case, experiments are repeated five times. During the experiments, the user is conducted to draw continuous and

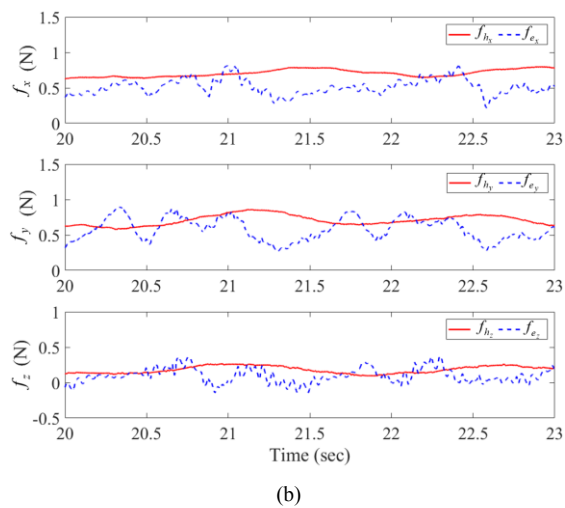
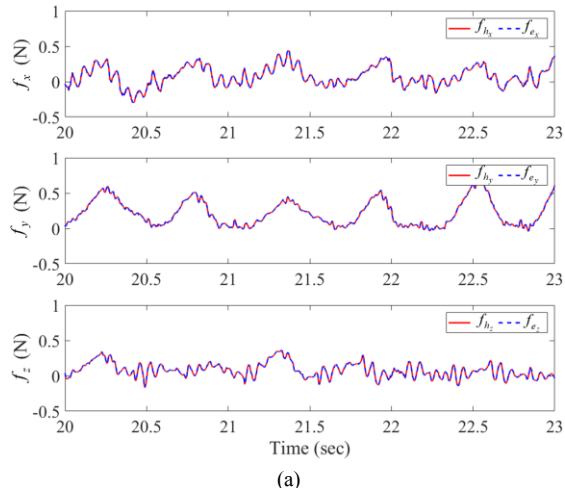


Figure 7. Contact force results of the master (red solid line,  $f_h$ ) and slave (blue dashed line,  $f_e$ ) robots in 3D for the cases (a) without motion compensation and (b) with motion compensation. Subscripts  $i = x, y, z$  are the three axes, respectively.

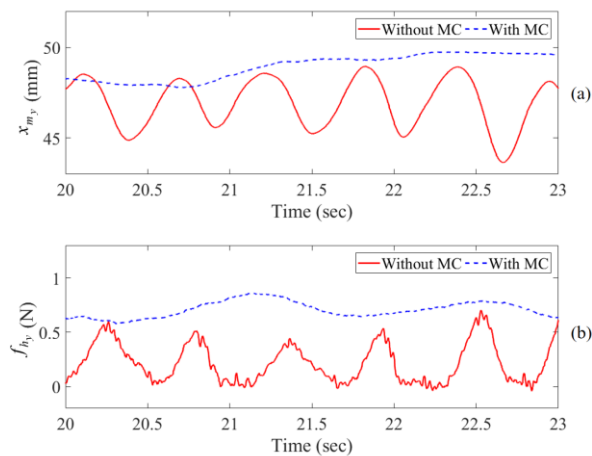


Figure 8. (a) Positions and (b) forces of the master robot in the  $y$ -axis for the two cases. Legend MC is the abbreviation of motion compensation.

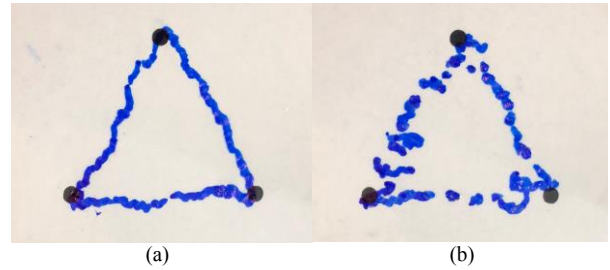


Figure 9. Triangle results. (a) With motion compensation. (b) Without motion compensation.

straight lines and at the same time to finish the task as soon as possible.

Based on the results shown in Table II and Fig. 7, it can be concluded that with motion compensation the master position will be steadier than the slave position, and without motion compensation, the master position will be the same as the slave position. Therefore, the motion commands of the human operator for the two cases are not shown. Fig. 9 shows representative drawn triangle results for the two cases. With motion compensation (Fig. 9a), the drawn lines are more continuous and straighter than the without motion compensation (Fig. 9b). The latter has break points and is fragmented. Under motion compensation, task completion times ( $56.38 \pm 4.33s$ ) are shorter than without motion compensation ( $77.09 \pm 4.72s$ ) by as much as 25%. The t-test  $p$ -value, 0.026, ensures a statistically significant difference between the task completion times under two cases (significance corresponds to  $p < 0.05$ ). The results of usability study present the dominant advantage of the proposed control system over the direct force reflection system. Although the triangle is drawn on a plane, considering the 3D motion of the heart surface (the plane), the task is 3D.

#### D. Discussion

The experimental position results show that the position tracking performance of the slave robot improves significantly when using the proposed semi-autonomous surgical robot control system. When there is no motion compensation (as can be seen in Fig. 6(a) and Fig. 8(a)), manually compensating for the complex 3D heart motion is not accurate or comfortable for the human operator. In this case, the human operator needs not only compensate for the heart motion but also perform task on the heart tissue, which requires high focus and is very easy to cause fatigue. On the contrary, with motion compensation, the MASE is roughly 60% less than that the case without motion compensation. The slave robot complies with the heart motion automatically and the human operator (shown in Fig. 8(a)) only provides position commands to the slave robot and does not need to move back and forth to mimic the heart motion, which is more convenient for the operator to implement surgical tasks.

The force results also demonstrate that the force feedback to the human operator is non-oscillatory by using the proposed method. When using direct force reflection method, in order to reduce the tool-tissue collision and tissue injury, the human operator in the experiments pays more attention to motion compensation but constant contact which is more challenging. This leads to contact discontinuity as the slave robot is very easy to be bounced off the heart surface. When using the

proposed method, the slave robot can be easily controlled to stay in constant contact with the heart surface because the human operator only needs to focus on the contact task regardless of the fast motion of the heart. The designed reference impedance model for the master robot guarantees the force feedback to the human operator is relatively steady.

## V. CONCLUSION

A semi-autonomous surgical robot control system is proposed for 3D physiological motion compensation and non-oscillatory haptic feedback in beating-heart surgery. The proposed method only uses the measured interaction forces without any need for vision-based heart motion estimation, active observer or motion prediction to compensate for the beating-heart motion automatically and provide the human operator with a feeling of operating on a stabilized heart simultaneously. The experimental evaluation demonstrated that the proposed method could be used in the robot with significant dynamics and achieve accurate performance. Future work may involve exploring the system's potential uses in forms of beating-heart procedures.

## ACKNOWLEDGEMENTS

This work is supported by the Canada Foundation for Innovation (CFI) under grant LOF 28241 and JELF 35916, the Alberta Innovation and Advanced Education Ministry under Small Equipment Grant RCP-12-021, the Alberta Innovation and Advanced Education Ministry under Small Equipment Grant RCP-17-019, the Natural Sciences and Engineering Research Council (NSERC) of Canada under grant RGPIN 372042, the Natural Sciences and Engineering Research Council (NSERC) of Canada under grant RGPIN 03907, and the China Scholarship Council (CSC) under grant [2015]08410152.

## REFERENCES

- [1] D. Paparella, T. M. Yau, and E. Young, "Cardiopulmonary bypass induced inflammation: Pathophysiology and treatment. An update," *Eur. J. Cardio-thoracic Surg.*, vol. 21, no. 2, pp. 232–244, 2002.
- [2] B. Fei, W. Sing, S. Chauhan, and C. Keong, "The safety issues of medical robotics," *Reliab. Eng. Syst. Saf.*, vol. 73, pp. 183–192, 2001.
- [3] S. G. Yuen, N. V. Vasilyev, J. Pedro, and R. D. Howe, "Robotic Tissue Tracking for Beating Heart Mitral Valve Surgery," *Med. Image Anal.*, vol. 17, no. 8, pp. 1236–1242, 2013.
- [4] S. B. Kesner and R. D. Howe, "Robotic catheter cardiac ablation combining ultrasound guidance and force control," *Int. J. Rob. Res.*, vol. 33, no. 4, pp. 631–644, 2014.
- [5] P. Moreira, N. Zemiti, C. Liu, and P. Pognet, "Viscoelastic model based force control for soft tissue interaction and its application in physiological motion compensation," *Comput. Methods Programs Biomed.*, vol. 116, no. 2, pp. 52–67, 2014.
- [6] B. Cagneau, N. Zemiti, D. Bellot, and G. Morel, "Physiological Motion Compensation in Robotized Surgery using Force Feedback Control," in *Proceedings 2007 IEEE International Conference on Robotics and Automation*, pp. 1881–1886, 2007.
- [7] I. Paranawithana *et al.*, "Ultrasound – Guided Involuntary Motion Compensation of Kidney Stones in Percutaneous Nephrolithotomy Surgery," in *IEEE 14th International Conference on Automation Science and Engineering (CASE)*, pp. 1123–1129, 2018.
- [8] Y. Nakamura, K. Kishi, and H. Kawakami, "Heartbeat synchronization for robotic cardiac surgery," *Proc. - IEEE Int. Conf. Robot. Autom.*, vol. 2, pp. 2014–2019, 2001.
- [9] Y. Nakajima, T. Nozaki, and K. Ohnishi, "Heartbeat synchronization with haptic feedback for telesurgical robot," *IEEE Trans. Ind. Electron.*, vol. 61, no. 7, pp. 3753–3764, 2014.
- [10] S. Mansouri, F. Farahmand, G. Vossoughi, and A. A. Ghavidel, "A Hybrid Algorithm for Prediction of Varying Heart Rate Motion in Computer-Assisted Beating Heart Surgery," *J. Med. Syst.*, vol. 42, no. 10, 2018.
- [11] E. E. Tuna, T. J. Franke, O. Bebek, A. Shiose, K. Fukamachi, and M. C. Çavuşoğlu, "Heart Motion Prediction Based on Adaptive Estimation Algorithms for Robotic Assisted Beating Heart Surgery," *IEEE Trans. Robot.*, vol. 29, no. 1, pp. 261–276, 2013.
- [12] E. E. Tuna, J. H. Karimov, T. Liu, Ö. Bebek, K. Fukamachi, and M. C. Çavuşoğlu, "Towards active tracking of beating heart motion in the presence of arrhythmia for robotic assisted beating heart surgery," *PLoS One*, vol. 9, no. 7, p. e102877(1-8), 2014.
- [13] M. Bowthorpe, M. Tavakoli, H. Becher, and R. Howe, "Smith predictor-based robot control for ultrasound-guided teleoperated beating-heart surgery," *IEEE J. Biomed. Heal. Informatics*, vol. 18, no. 1, pp. 157–166, 2014.
- [14] M. Bowthorpe and M. Tavakoli, "Generalized Predictive Control of a Surgical Robot for Beating-Heart Surgery Under Delayed and Slowly-Sampled Ultrasound Image Data," *IEEE Robot. Autom. Lett.*, vol. 1, no. 2, pp. 892–899, 2016.
- [15] L. Cheng and M. Tavakoli, "Ultrasound image guidance and robot impedance control for beating-heart surgery," *Control Eng. Pract.*, vol. 81, pp. 9–17, 2018.
- [16] L. Cheng, M. Sharifi, and M. Tavakoli, "Towards robot-assisted anchor deployment in beating-heart mitral valve surgery," *Int. J. Med. Robot. Comput. Assist. Surg.*, vol. 14, no. 3, pp. 1–10, 2018.
- [17] L. Cheng and M. Tavakoli, "Switched-Impedance Control of Surgical Robots in Teleoperated Beating-Heart Surgery," *J. Med. Robot. Res.*, no. March, p. 1841003, 2018.
- [18] R. Cortesão and M. Dominici, "Robot Force Control on a Beating Heart," *IEEE/ASME Trans. Mechatronics*, vol. 22, no. 4, pp. 1736–1743, 2017.
- [19] A. Ruskowski, C. Schneider, O. Mohareri, and S. Salcudean, "Bimanual Teleoperation with Heart Motion Compensation on the da Vinci R Research Kit: Implementation and Preliminary Experiments," in *Proceedings - IEEE International Conference on Robotics and Automation*, pp. 4101–4108, 2016.
- [20] R. Richa, A. P. L. Bó, and P. Pognet, "Beating heart motion prediction for robust visual tracking," *2010 IEEE Int. Conf. Robot. Autom.*, pp. 4579–4584, 2010.
- [21] B. Yang, C. Liu, W. Zheng, and S. Liu, "Motion prediction via online instantaneous frequency estimation for vision-based beating heart tracking," *Inf. Fusion*, vol. 35, no. September, pp. 58–67, 2016.
- [22] R. Richa, P. Pognet, and C. Liu, "Three-dimensional Motion Tracking for Beating Heart Surgery Using a Thin-plate Spline Deformable Model," *Int. J. Rob. Res.*, vol. 29, no. 2, pp. 218–230, 2010.
- [23] J. Fong, "Kinesthetic Teaching of a Therapist's Behavior to a Rehabilitation Robot," *2018 Int. Symp. Med. Robot.*, pp. 1–6.
- [24] M. Tavakoli, R. V. Patel, M. Moallem, and A. Aziminejad, *Haptics for Teleoperated Surgical Robotic Systems*. World Scientific Publishing Co., Inc., 2008.
- [25] S. B. Kesner and R. D. Howe, "Discriminating Tissue Stiffness with a Haptic Catheter: Feeling the Inside of the Beating Heart," in *IEEE World Haptics Conference*, pp. 1–6, 2011.